Journal of Marine Research, 53, 571–607, 1995

Parameter optimization and analysis of ecosystem models using simulated annealing: A case study at Station P

by Richard J. Matear[1]

ABSTRACT

A simulated annealing optimization algorithm is formulated to optimize parameters of ecosystem models. The optimization is used to directly determine the model parameters required to reproduce the observed data. The optimization routine is formulated in a general manner and is easily modified to include additional information on both the desired model output and the model parameters. From the optimization routine, error analysis of the optimal parameters is provided by the error-covariance matrix which gives both the sensitivity of the model to each model parameter and the correlation coefficients between all pairs of model parameters. In addition, the optimization analysis provides a means of assessing the necessary model complexity required to model the available data.

To demonstrate the technique, optimal parameters of three different ecosystem model configurations are determined from nitrate, phytoplankton, mesozooplankton and net phytoplankton productivity measurements at Station P. At Station P, error analysis of the optimal parameters indicates that the data are able to resolve up to 10 independent model parameters. This is always less than the number of unknown model parameters indicating that the optimal solutions are not unique. A simple nitrate-phosphate-zooplankton ecosystem is successful at reproducing the observations. To justify the use of a more complicated model at Station P requires additional data to constrain the optimization routine. Although there is evidence supporting the importance of the microbial loop at Station P, without additional ammonium and bacteria measurements one cannot validate a more complicated model that includes these processes.

1. Introduction

An important question in oceanographic research involves understanding the relationship between physical oceanography and the marine ecosystem. To assess the future uptake of anthropogenic CO_2 by the ocean, one will need to assess how the marine ecosystem will respond to changes in the ocean circulation produced by changes in the physical forcing functions (i.e. solar radiation and the wind field) due to climate change. Previous box modeling studies show that the air-borne fraction of CO_2 is strongly affected by changes in the ocean biological pump (Sarmiento *et al.,* 1989; Peng and Broecker, 1991; Joos *et al.,* 1991). Simple ecosystem models provide a

1. Centre for Ocean Climate Chemistry, Institute of Ocean Sciences, P.O. Box 6000, 9860 W. Saanich Rd., Sidney, BC, Canada V8L 4B2.

valuable tool for understanding the interaction between the forcing functions and the ecosystem.

In recent years, 1-D ecosystem models have been used to trace the flow of material between various components in an ecosystem (Evans and Parslow, 1985; Frost, 1987; Fasham *et al.,* 1990; Radach, 1993). To apply these models, a large number of parameters must be specified. To assign values to the biological parameters is especially difficult, because unlike many chemical or physical parameters, they cannot be regarded as constants (Fasham *et al.,* 1990). This problem has been approached by using an optimization technique to determine model parameters from the data. This *inverse* formalism provides a means of producing a set of ecosystem model parameters that is most consistent with the available information. It is a natural way of objectively assigning values to the model parameters. Inverse methods have been applied to observations to quantify the steady-state flow of nitrogen and carbon between the various components of the ecosystem model (Vézina and Platt, 1988; Vézina, 1989; Jackson and Eldridge, 1992). In all these references, a linear inverse problem was formulated to quantify the mean steady-state flow of nitrogen and carbon between various components in the model. Inverse techniques will be applied to a more complicated non-linear problem of modeling the seasonal cycle of the plankton dynamics.

For ecosystem models like Evans and Parslow (1985) or Fasham *et al.* (1990), the large number of model parameters and the non-linearity of the ecosystem model make it difficult to evaluate the sensitivity of the model to the various parameters. Inverse methods provide a natural way of exploring the parameter space of an ecosystem model to determine sensitivity of the ecosystem model to the model parameters and to investigate the correlation between the various model parameters.

The techniques presented in this paper provide a novel and general way of incorporating field measurements into an ecosystem model. The primary focus of this paper is to illustrate the use of an optimization technique to analyze ecosystem models. One which would determine the essential dynamics of the ecosystem model reflected in the available data and explore the parameter space of the model. To demonstrate the technique, data collected from Station P in the subarctic Pacific were used to optimally estimate model parameters of three different ecosystem model configurations. Section 2 provides a description of the different ecosystem models used. Section 3 describes the data from Station P used to force the ecosystem model and to constrain the model parameters. In Section 4, the optimization problem is outlined and a brief synopsis of the simulated annealing routine is presented. The advantages and disadvantages of the simulated annealing are discussed and the performance of simulated annealing is compared to the conjugate gradient algorithm. In Section 5, the results of the optimization of the three different

ecosystem model configurations at Station P are presented. Section 6 discusses and summarizes the results of this study.

2. Ecosystem model

a. Model structure

Following the suggestion of Platt *et al.* (1981), three different ecosystem model configurations were formulated to assess the necessary model complexity required to reproduce the observations. These models served to encompass the general knowledge of the biological conditions in the oceans. All three model configurations described the seasonal variation of the phytoplankton biomass and production at a point in the ocean. In all the models, horizontal advection and diffusion were ignored and the pelagic ecosystem was assumed to consist of a homogeneous mixed layer overlying a deeper abiotic layer (Steele, 1974). The phytoplankton and zooplankton were assumed to be confined and homogeneously distributed in the upper layer.

These models have been used to model biological conditions in the Pacific and Atlantic oceans. In applying these models at Station P, Frost (1991) showed that the effect of ignoring horizontal advection and diffusion were small. Confining the phytoplankton and zooplankton to the mixed layer at Station P was an oversimplification, but eliminated the need for detailed parameterization of mixing and plankton growth, grazing and mortality within the pycnocline. This simplification underestimated the integrated water column primary production at Station P in the summer when the significant amount of chlorophyll *a* can be found below the mixed layer (Anderson *et al.,* 1977).

For all three configurations, the mixed layer dynamics were not explicitly modeled, rather observed mixed layer depths were used to describe the temporal evolution of the mixed layer depth (H)

$$\frac{dH}{dt} = \zeta(t). \tag{1}$$

Following Evans and Parslow (1985), changes in the mixed layer had an asymmetrical effect on the model depending on whether a component was motile or not. Only the zooplankton in the model were assumed able to maintain their position in the mixed layer, therefore were concentrated as the mixed layer shallowed. A shallowing of the mixed layer ($\zeta < 0$) introduced no new water into the mixed layer and the concentrations of nitrate, phytoplankton and other non-motile components remained constant in the mixed layer. Only the deepening of the mixed layer ($\zeta > 0$) generated mixing with the water underlying the mixed layer to produce changes in the concentrations of nitrate, phytoplankton and other non-motile components in the mixed layer. To capture this assymmetry in the model, one defines $\zeta^+(t) = \max(\zeta(t), 0)$ (Evans and Parlsow, 1985).

For all three configurations, the temporal evolution of the different components of the models was in units of μM N.

i. 3-component model. The first ecosystem model configuration modeled the nitrate (N), phytoplankton (P) and zooplankton (Z) concentration in the mixed layer. The model was based on the Evans and Parslow (1985) model with the modification that a fraction of the grazed phytoplankton and of the zooplankton mortality were returned directly to the nitrate component. The equations for the temporal evolution of nitrate, phytoplankton and zooplankton concentrations were

$$\frac{dN}{dt} = -[\sigma(t,H)Q_1 - \mu_1]P + \frac{m + \zeta^+(t)}{H}(N_o - N) + (1 - \gamma_2)\gamma_5 \frac{g(P - P_o)Z}{K_3 + P - P_o} + (1 - \gamma_4)\mu_5 Z \tag{2}$$

$$\frac{dP}{dt} = [\sigma(t,H)Q_1 - \mu_1]P - \frac{g(P - P_o)Z}{K_3 + P - P_o} - \frac{m + \zeta^+(t)}{H}P \tag{3}$$

$$\frac{dZ}{dt} = \frac{\gamma_2 g(P - P_o)Z}{K_3 + P - P_o} - \mu_5 Z - \frac{\zeta(t)}{H}Z \tag{4}$$

where N_o was the nitrate concentration one meter below the depth of the mixed layer. For the phytoplankton growth rate, the non-dimensional nutrient limitation term was

$$Q_1 = \frac{N}{K_1 + N}. \tag{5}$$

The light-limited growth rate, in units of d^{-1}, averaged over the depth of the mixed layer was obtained by integrating over one day/night cycle

$$\sigma(t,H) = 2\frac{1}{H}\int^{\tau}\int^{H} F(I)\,dz\,dt \tag{6}$$

where $F(I)$ was a function describing the phytoplankton photosynthesis-irradiance relationship (the P-I curve), 2τ was the day-length (calculated from Brock, 1981) and I was the photosynthetically active radiation (PAR) as a function of depth below the surface of the water. The function $F(I)$ was defined by the Smith function (Smith, 1936)

$$F(I) = \frac{V_p(T)\alpha I}{(V_p(T) + \alpha^2 I^2)^{1/2}} \tag{7}$$

where V_p was the growth rate as $I \to \infty$ and α was the initial slope of the *P-I* curve. The maximum temperature-dependent growth was defined following Eppley (1972)

$$V_p(T) = 0.6(1.066)^T \tag{8}$$

and light intensity at any depth was given by

$$I(z, t) = PAR \qquad I(0, t) \exp\left(-k_w z - \int_0^z k_c P dz\right) \tag{9}$$

where $I(0,t)$ was the incident radiation observed immediately below the surface of the water, *PAR* was the photosynthetically active radiation, z was depth in meters; P was the concentration of phytoplankton in the mixed layer, the k_w and k_c were light attenuation constants with typical values of $0.04\ m^{-1}$ and $0.06\ (\mu M\ m^{-3})^{-1}\ m^{-1}$ respectively (Evans and Parslow, 1985). The variation of $I(0, t)$ with time was assumed to be triangular which allowed one to analytically integrate Eq (6) (Evans and Parslow, 1985).

As described above, the ecosystem model required 14 model parameters (Table 1).

ii. 4-component model. The second model configuration separated the zooplankton component of the 3-component model into two size classes—microzooplankton (Z) and mesozooplankton (M). This was based on modeling work by Frost (1987) which showed that only the microzooplankton have the potential grazing capacity to prevent a bloom of phytoplankton. The model was identical to the previously discussed 3-component ecosystem model with the inclusion of the mesozooplankton. The grazing by the mesozooplankton was parameterized following the work of Frost (1987), however in this model mesozooplankton was explicitly modeled. The equations for this model were

$$\frac{dN}{dt} = -[\sigma(t, H)Q_1 - \mu_1]P + \frac{m + \zeta^+(t)}{H}(N_o - N) + (1 - \gamma_2)\gamma_5 \frac{g(P - P_o)Z}{K_3 + P - P_o} + (1 - \gamma'_2)\gamma'_5 \frac{g'(Z + P)M}{K'_3 + P + Z} + (1 - \gamma'_4)\mu'_5 M \tag{10}$$

$$\frac{dP}{dt} = [\sigma(t, H)Q_1 - \mu_1]P - \frac{g(P - P_o)Z}{K_3 + P - P_o} - \frac{m + \zeta^+(t)}{H}P - \frac{g'PM}{K_3 + P + Z} \tag{11}$$

$$\frac{dZ}{dt} = \frac{\gamma_2 g(P - P_o)Z}{K_3 + P - P_o} - \frac{\zeta(t)}{H}Z - \frac{g'ZM}{K_3 + P + Z} \tag{12}$$

$$\frac{dM}{dt} = \mu'_5 M - \frac{\zeta(t)}{H}M - \frac{\gamma'_2 g'(Z + P)M}{K'_3 + P + Z}. \tag{13}$$

Table 1. A list of different model parameters required by the ecosystem models. The uncertainty in the *a priori* value was used by the optimization scheme (see text) and if an uncertainty was not provided then the corresponding parameter was assumed to be specified. A check mark in the last three columns indicates whether the parameter was required by the 3-, 4- or 7-component model.

	Symbol	*A priori* value	Units	3	4	7
Phytoplankton (P) parameters						
Exudation fraction	$\gamma 1$	0.05 ± 0.01				✓
Specific mortality rate	$\mu 1$	0.024 ± 0.05	d^{-1}	✓	✓	✓
Half Saturation constant for nutrient uptake	K_1, K_2	1.0 ± 1.0	μM	✓	✓	✓
Ammonium inhibition parameter	Ψ	1.5	$(\mu M)^{-1}$			✓
Light attenuation by phytoplankton	K_c	0.06	$m^{-1}(\mu M)^{-1}$	✓	✓	✓
Light attenuation by water	K_w	0.04	m^{-1}	✓	✓	✓
Initial Slope of P-I curve	α	0.025 ± 0.01	$(W\ m^{-2}\ d)^{-1}$	✓	✓	✓
Photosynthetically active radiation	PAR	0.5		✓	✓	✓
Zooplankton (Z) and Mesozooplankton (M)parameters						
Assimilation efficiency of Z	γ_2	0.5 ± 0.1		✓	✓	✓
Ammonium fraction of Z excretion	γ_3	0.75 ± 0.3				✓
Detrial fraction of Z mortality	γ_4	0.33 ± 0.1		✓		✓
Fraction of Z grazing excreted as nitrogen metabolites	γ_5	0.6 ± 0.05		✓	✓	
Specific excretion rate of Z	μ_2	0.1 ± 0.5	d^{-1}			✓
Specific mortality rate of Z	μ_5	0.07 ± 0.02	d^{-1}	✓		✓
Maximum growth rate of Z	g	1.0 ± 0.2	d^{-1}	✓	✓	✓
Half Saturation for ingestion of Z	K_3	0.5 ± 0.3	μM	✓	✓	✓
Grazing threshold of Z	P_o	0.05 ± 0.05	μM	✓	✓	
Relative preference for phyto-plankton of Z	p_1	0.35 ± 0.1				✓
Relative preference for bacteria of Z	p_2	0.45 ± 0.1				✓
Relative preference for PON of Z	p_3	0.2 ± 0.1				✓
Detrital fraction of M mortality	γ_4'	0.33 ± 0.1			✓	
Specific mortality rate of M	μ_5'	0.05 ± 0.02	d^{-1}		✓	
Maximum growth rate M	g'	0.3 ± 0.1	d^{-1}		✓	
Assimilation efficiency of M	γ_2'	0.5 ± 0.1			✓	
Specific excretion rate of M	γ_5'	0.6 ± 0.05			✓	
Half Saturation for ingestion by M.	K_3'	0.9 ± 0.1	μM		✓	
Bacteria (B) parameters						
Specific excretion rate	μ_3	0.05 ± 0.025	d^{-1}			✓
Maximum growth rate	V_b	2.0 ± 0.5	d^{-1}			✓
Half Saturation for uptake	K_4	0.5 ± 0.2	μM			✓
Ammonium/dissolved organic nitrogen uptake ratio	η	0.6 ± 0.2				✓
Detrial (N_p)parameters						
Breakdown rate	μ_4	0.05 ± 0.2	d^{-1}			✓
Sinking velocity	w_s	10.0 ± 3.0	$m\ d^{-1}$			✓
Physical Mixing parameters						
Diffusion Rate	m	3.0 ± 0.5	$m\ d^{-1}$	✓	✓	✓
Total Number of model parameters				14	18	25

The daily growth rate of phytoplankton was as defined in the 3-component model. This model required 18 model parameters (Table 1).

iii. 7-component model. The third model configuration was based on the model presented by Fasham *et al.* (1990) which included the microbial loop. The application of this model was motivated by work by Azam *et al.* (1983) which showed that the microbial loop plays an important role in the plankton dynamics in the northeast Pacific Ocean. The model components were nitrate (N_n), phytoplankton (P), zooplankton (Z), bacteria (B), particulate organic nitrogen, (N_p), dissolved organic nitrogen (N_d) and ammonium (N_r) (Fasham *et al.*, 1990). The model equations are presented below; for a more complete description of the model refer to Fasham *et al.* (1990).

$$\frac{dN_n}{dt} = -\sigma(t, M)[Q_1(N_n, N_r)]P + \frac{m + \zeta^+(t)}{M}(N_n - N_o) \tag{14}$$

$$\frac{dP}{dt} = (1 - \gamma_1)\{\sigma(t, M)[Q_1(N_n, N_r) + Q_2(N_r)]P\} - G_1 - \mu_1 P - \frac{m + \zeta^+(t)}{M}P \tag{15}$$

$$\frac{dZ}{dt} = \gamma_2[G_1 + G_2 + G_3] - [\mu_2 + \mu_5]Z - \frac{\zeta^+(t)}{M}Z \tag{16}$$

$$\frac{dB}{dt} = [U_1 + U_2] - G_2 - \mu_3 B - \frac{m + \zeta^+(t)}{M}B \tag{17}$$

$$\frac{dN_p}{dt} = \mu_1 P - G_3 - \mu_4 N_p + (1 - \gamma_2)(G_1 + G_2 + G_3) - \frac{m + \zeta^+(t) + w_s}{M}N_p \tag{18}$$

$$\frac{dN_r}{dt} = -\sigma(t, M)[Q_2(N_r)]P - U_2 + \mu_3 B + [\gamma_3\mu_2 + (1 - \gamma_4)\mu_5]Z - \frac{m + \zeta^+(t)}{M}N_r \tag{19}$$

$$\frac{dN_d}{dt} = [(1 - \gamma_3)\mu_2 Z + \mu_4 N_p - U_1 + \gamma_1\sigma(t, M)[Q_1(N_n, N_r) + Q_2(N_r)]P - \frac{m + \zeta^+(t)}{M}N_d. \tag{20}$$

The light-limited growth term was as defined in the 3-component model. The non-dimensional nutrient limitation terms for ammonium and nitrate were

$$Q_1(N_n, N_r) = \frac{N_n}{K_1 + N_n} e^{-(\Psi N_r)} \tag{21}$$

$$Q_2(N_r) = \frac{N_r}{K_2 + N_r}. \tag{22}$$

The zooplankton grazing rates (in μM N d^{-1}) were defined by the following equation

$$G_j = gZ \frac{pj C_j^2}{K_g \sum_{k=1}^{3} pk C_k + \sum_{k=1}^{3} pk C_j^2} \quad j = 1 \ldots 3 \tag{23}$$

where $C_1 = P$, $C_2 = B$, and $C_3 = N_p$.

Bacterial uptake of nitrogen in μM N d^{-1} was defined by the following equations

$$U_1 = \frac{V_b N_d B}{K_4 + S + N_d} \tag{24}$$

$$U_2 = \frac{V_b S B}{K_4 + S + N_d} \tag{25}$$

$$S = \min(N_r, \eta N_d). \tag{26}$$

This model required 25 model parameters (Table 1).

b. Model numerics

The full set of differential equations describing the ecosystem model was solved using a fourth-order Runge-Kutta algorithm. Testing of the algorithm showed that a one day time step was sufficient to produce accurate estimates of the concentration of the modeled components. The simulations were run for three years and a day, with the third year of data being used by the optimization routine. Typically by the third year, the model achieved a steady state annual cycle which was not sensitive to the initial conditions. At steady-state, the concentrations of the modeled components on the first day of the third year were identical to the concentrations on the first day of the fourth year.

3. Data from Station P

A large amount of data on biological, chemical and physical oceanography is available from Station P and the data used in this study are summarized in Table 2. For this study, the data sets are separated into data used to force the model and data used to constrain the model parameters.

Table 2. Datasets available at Station P used to force the ecosystem model to constrain optimization and to evaluate the ecosystem model output.

Dataset	Reference
Monthly incident radiation	Dobson and Smith, 1985
Daily mixed layer depth and temperature	Tabata (personal communication)
Seasonal cycle of nitrate	Wong, (unpublished data)
Seasonal cycle of phytoplankton biomass	Anderson *et al.*, 1977
Depth distribution of phytoplankton	Anderson *et al.*, 1977
Monthly primary production observations	McAllister, 1969; Parslow, 1981
Seasonal zooplankton biomass (meso-zooplankton)	McAllister, 1969; LeBrasseur and Kennedy, 1972; Miller *et al.*, 1984;
Monthly estimates of new production	Wong, (unpublished data); Wheeler and Kokkinakis, 1992
Bacterial nitrogen	Simon *et al.*, 1992
Surface ammonium concentration	Wheeler and Kokkinakis, 1990

a. Forcing data

The forcing terms of the ecosystem model were the annual cycles of solar radiation, mixed layer depth, mixed layer temperature and nitrate concentration below the mixed layer. Data for these variables were based on averages of observations made at Station P (see Table 2 for references).

Mean monthly values of total solar radiation at Station P for the period of 1959 to 1975 are reported by Dobson and Smith (1985). Their data were interpolated to daily values of the mean incident solar radiation (Fig. 1a). The daily mean solar radiation measurements were converted to peak values for noon by assuming the daily variation in light intensity was triangular. The photosynthetically active radiation (*PAR*) just below the surface at noon was assumed to be a constant fraction of the incident solar radiation. In reality, the ratio of PAR to total radiation is affected by sun zenith angle, water vapor content and aerosol optical thickness (Baker and Frouin, 1987). However, such complications were unnecessary for the scope of the present study and a constant value was used.

Seasonal variations in the mixed layer depth (Fig. 1b) were based on the average mixed layer depth observed at Station P between 1970 and 1980. The daily changes in the mixed layer depth, calculated from finite center differencing of Figure 1b, determined the amount of entrainment or detrainment occurring at the base of the mixed layer (Fig. 1c). The high frequency variability observed in Figure 1c reflects the importance of episodic events on the temporal evolution of the mixed layer (Large *et al.*, 1986), which was still evident after averaging eleven years of data. The average mixed layer temperatures for this period of time were determined by integrating the observed temperature measurements over the depth of the mixed layer (Fig. 1d). The empirical relationship between phytoplankton maximum growth rate and temperature derived by Eppley (1972) was used to determine the maximum growth rate of phytoplankton in the mixed layer.

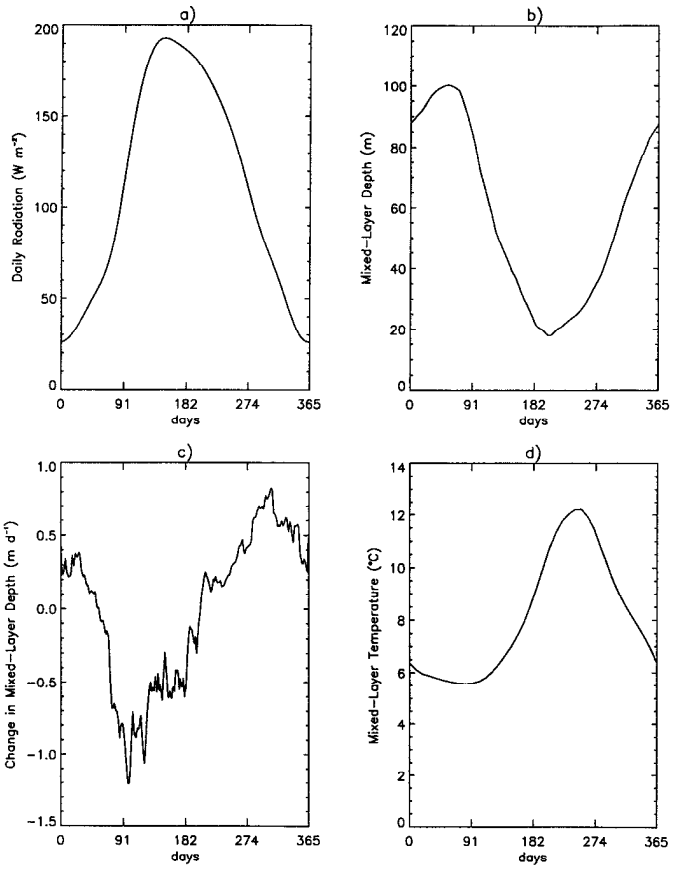

Figure 1. Observations from Station P for (a) daily incident solar radiation, (b) depth of the mixed layer (m), (c) the rate of the change of the mixed layer depth (m d^{-1}), and (d) temperature of the mixed layer (°C).

Nitrate concentrations collected from Station P for the period of 1970 to 1981 provide a good sampling of the nitrate concentration in the upper ocean. From this data, the annual cycle of nitrate concentration in the upper ocean was produced (Fig. 2). Using the data in Figure 2, the nitrate concentrations below the mixed layer were set to the nitrate concentration 1 m below the depth of the mixed layer (Fig. 3).

b. Constraining the parameter optimization

To apply the parameter optimization, one must provide information that describes the relevant features desired in the model output (constraints). These constraints are then used by the optimization routine to determine the model parameters that best satisfy these constraints. The data available at Station P to constrain the model were

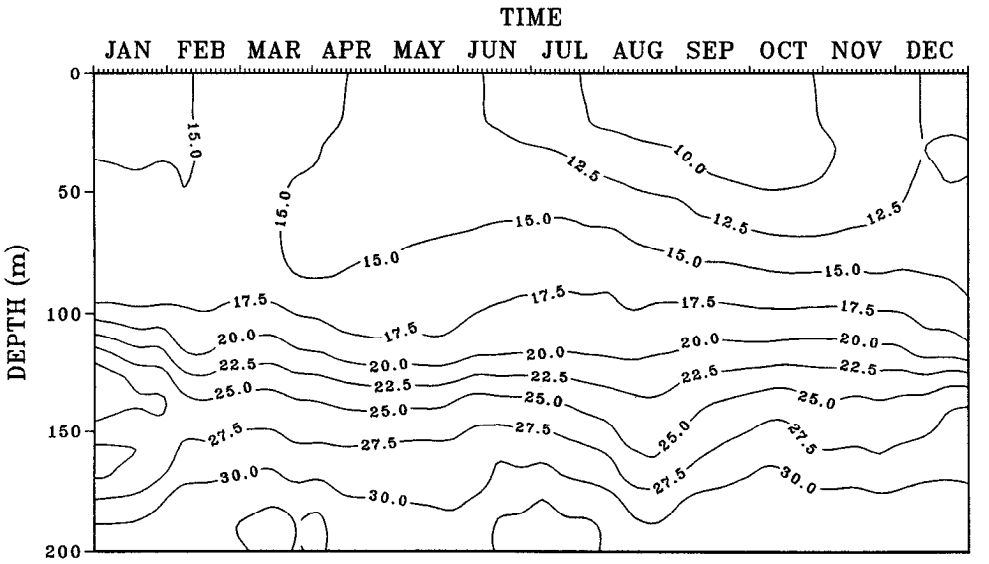

Figure 2. Average seasonal cycle of nitrate concentration in the upper ocean at Station P in μM.

nitrate, phytoplankton, mesozooplankton concentrations in the mixed layer and net phytoplankton productivity (NPP) from the mixed layer.

Integration of Figure 2 over the observed mixed layer depths produced the values of the observed nitrate concentration in the mixed layer (Fig. 3). The nitrate concentration in the mixed layer at station P was relatively high with the seasonal cycle varying between 9 μM and 16 μM. Estimate of the errors associated with the data were determined from the standard deviation of the surface nitrate concentration from the seasonal mean and are shown in Figure 4a.

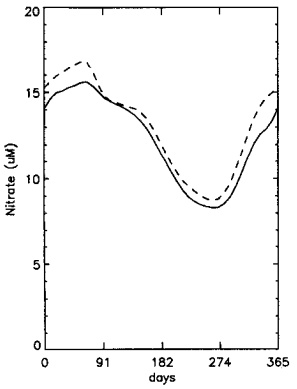

Figure 3. Nitrate concentration in μM for 1 m below the mixed layer (dashed), and for the mixed layer (solid).

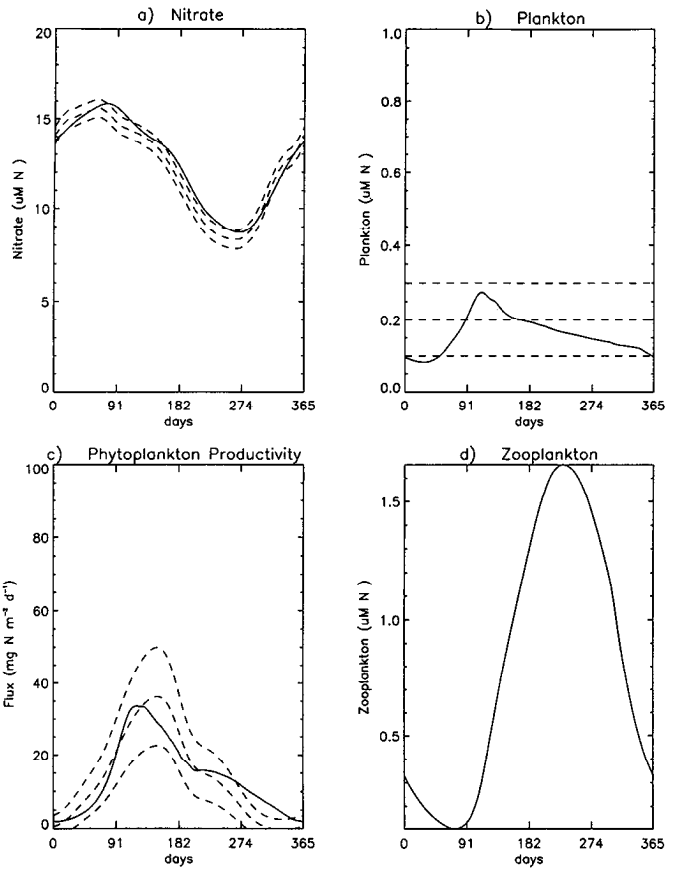

Figure 4. Reference run of the 3-component ecosystem model (model I) for the mixed layer (a) nitrate concentration, (b) phytoplankton concentration, (c) net phytoplankton productivity and (d) zooplankton concentration. The solid lines refer to the model and the three dashed lines are the data and the data with ± one standard deviations uncertainty.

A series of studies on the seasonal variation of the planktonic food web (McAllister, 1961; Stephens, 1964, 1966, 1968, 1970; Anderson *et al.*, 1977) have shown Station P to be atypical because of the absence of a spring bloom of phytoplankton (Fig. 5). This lack of phytoplankton blooms is evident from long-term sampling at Station P between 1950 and 1981. Throughout this period recurring spring blooms of phytoplankton were not observed and the blooms that did occur were small never exceeding 2 mg Chl *a* m^{-3}. For Station P the typical concentrations of phytoplankton for all seasons are between 0.3 and 0.4 mg Chl *a* m^{-3}. In contrast, in the subartic North Atlantic, even the most remote oceanic sites have phytoplankton blooms every year of greater than 1.0 mg Chl *a* m^{-3} (Parson and Lalli, 1988) when the major

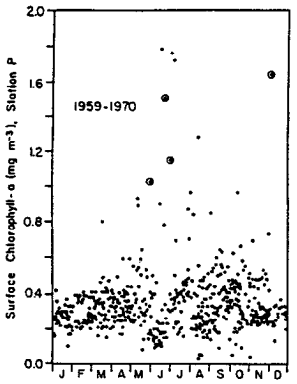

Figure 5. Chl *a* concentration measured at Station P, redrawn from Anderson (1977).

nutrient levels decrease to zero. Although there is no spring bloom at Station P, there is a spring peak in primary production followed by a summer peak in zooplankton biomass (Parslow, 1981). In general at Station P, the phytoplankton are uniformly distributed in the mixed layer and there is no subsurface maximum (Anderson *et al.*, 1977). For the model, the phytoplankton concentration was set to 0.15 μM ± 0.05 μM (mg C: mg Chl a = 50). The error reflected the uncertainty in the Chl *a* concentrations and the uncertainty in converting the phytoplankton Chl *a* concentration to a carbon and then nitrogen concentration.

The net phytoplankton productivity (NPP) was defined as the difference between the photosynthetic rate of phytoplankton minus the respiration rate of phytoplankton. Estimates of NPP are available at Station P over a period of several years (McAllister, 1969; and Parslow, 1981). To constrain the model, the estimated NPP of Parslow (1981) was used with a correction to account for the production occurring below the mixed layer in the summer (Fig. 4c). The differences between McAllister and Parslow estimates of NPP were used to assign the errors in the net phytoplankton productivity (δNPP) measurements (Fig. 4c).

At Station P, the standing stock of mesozooplankton vary seasonally in a fashion qualitatively similar to the cycle of primary production (Frost, 1987). From 1965 to 1980, the standing stocks of mesozooplankton were collected using vertical hauls of 150 m with a 350 μM mesh net (Fulton, 1983). A mean seasonal cycle of mesozooplankton standing stock at Station P was given by Miller *et al.* (1984). To constrain the optimization, the averaged nitrogen concentrations of mesozooplankton calculated by Frost (1987) for this data were used. The errors in the mesozooplankton concentrations were estimated from the difference between the two curves calculated by Frost (1987). The mesozooplankton concentrations, along with the prescribed errors, are shown in Figure 6d.

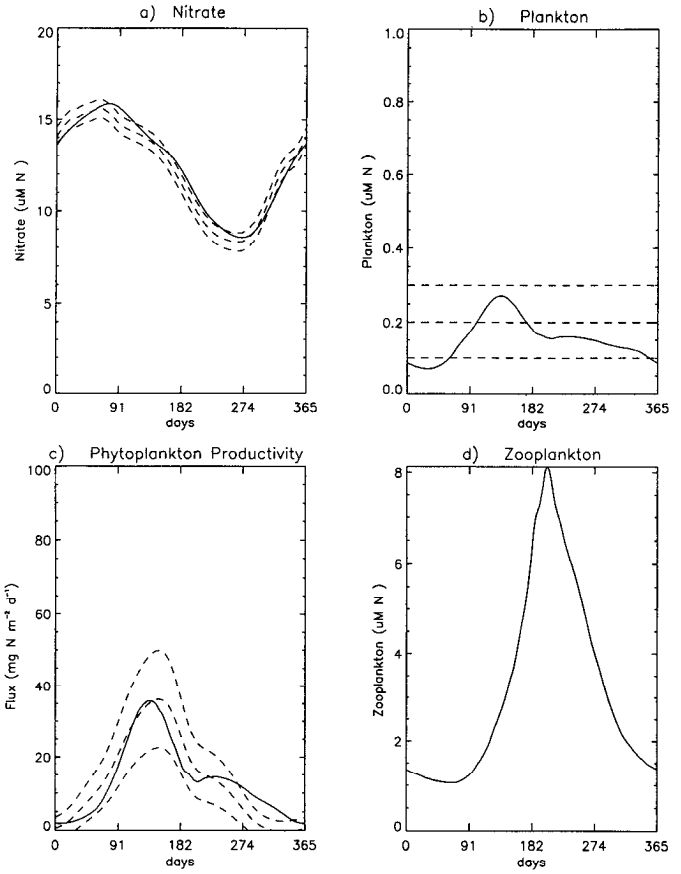

Figure 6. Reference run of the 4-component ecosystem reference model (model IV) for the mixed layer (a) nitrate concentration, (b) zooplankton concentration, (c) net phytoplankton productivity, (d) microzooplankton concentration, and (e) mesozooplankton concentration. The solid lines refer to the model and the three dashed lines are the data and the data with ± one standard deviations uncertainty.

4. Optimization problem

a. Implementation

The cost function was used to describe the desired features of the ecosystem model. For our optimization problem, the general cost function (J) was given by the following equation:

$$J = \frac{1}{2}\sum_{i=1}^{n}(N_i - N_i^*)^2\frac{1}{\delta N_i^2} + \frac{1}{2}\sum_{i=1}^{n}(P_i - P_i^*)^2\frac{1}{\delta P_i^2} + \frac{1}{2}\sum_{i=1}^{n}(NPP_i - NPP_i^*)^2\frac{1}{\delta NPP_i^2} + \frac{1}{2}\sum_{i=1}^{n}(M_i - M_i^*)^2\frac{1}{\delta M_i^2} + \frac{1}{2}\sum_{j=1}^{nc}(C_1^j - C_{366}^j)^4\frac{1}{\delta T^4} + \frac{1}{2}\sum_{i=1}^{m}(x_i - x_i^*)^2\frac{1}{\delta x_i^2} \quad (27)$$

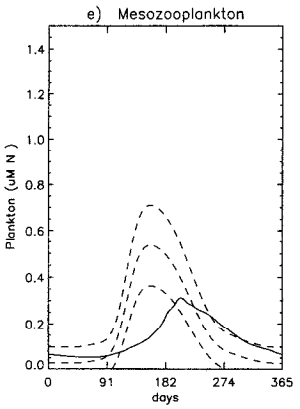

Figure 6. (Continued)

where N^*, P^*, NPP^* and M^* referred to the observations with prescribed uncertainties δN, δP, δNPP and δM; n referred to the number of data observations in a year ($n = 365$); nc referred to the number of components in the model; m referred to the number of model parameters; C^j referred to the different components in the model (i.e., N, P, Z, . . .); $\delta T = 0.01$ μM; and x referred to the model parameters. The cost function was composed of three penalty terms—data misfit penalty (terms 1–4), steady-state penalty (terms 5) and the *a priori* parameter penalty (term 6). The data misfit penalty required that the model output approximately reproduced the annual cycle of nitrate (N), phytoplankton (P), net primary productivity (NPP) and mesozooplankton (M). The steady-state penalty forced the model to produce a steady-state output with only a seasonal cycle, by requiring the model components at the start of the fourth year to be approximately equal to the values at start of the third year. The *a priori* parameter penalty on the values of the model parameters (x^*) incorporated information on the expected value of the model parameters. By setting δx_i in this penalty term to zero, one forced the value of x_i to be equal to the *a priori* value.

The *a priori* parameter penalty was included to try and force the model parameters to be within acceptable limits. The *a priori* values, along with their prescribed uncertainty, are given in Table 2. These values were derived from previous applications of the ecosystem models (Evans and Parslow, 1985; Frost, 1987; 1991; Fasham *et al.,* 1990). For easier comparison among the different ecosystem model configurations in this study, the parameters PAR, K_w and K_c were fixed at their *a priori* values.

b. Optimization algorithm

Simulated annealing was used to determine the optimal model parameters. The simulated annealing technique is well suited to handle optimization problems with strong non-linearity and a small number of unknown parameters (Kruger, 1993).

Algorithms associated with the name "simulated annealing" are stochastic and are based on the statistical model of the thermodynamic process for growing crystals. The simulated annealing method is analogous to the thermodynamics of the way liquid cools, freezes and crystallizes; that is, a perfect homogeneous crystal lattice represents a state of a solid material at a global minimum of energy. One method to obtain a nearly perfect crystal lattice is: (1) to heat the solid material up until it reaches an amorphous liquid state and then (2) cool the liquid very slowly using a specific scheme for decreasing temperature. The system will arrange itself into a state that closely resembles the structure of the perfect crystal at the global energy minimum, if the starting temperature is high enough to ensure nearly a random state and the cooling is slow enough to ensure thermal equilibrium at each temperature. As the system cools, each new configuration at a lower energy level than the previous one is unconditionally accepted by the system. However, in the thermodynamic system there is a non-vanishing probability related to the Boltzmann factor for a configuration at a higher energy level to be accepted.

The simulated annealing algorithm is the adaptation of the process described above to the problem of minimizing a function and was introduced by Kirkpatrick *et al.* (1983) as an optimization tool. To define the probability of accepting a higher cost function, a Metropolis function, $f(J_j, J_i, T)$, was used (Metropolis *et al.,* 1953).

$$f(J_j J_i T) = e^{\frac{-(J_j - J_i)}{T}} \tag{28}$$

where J_i is the current cost function, J_j is a new and higher cost function and T is a control parameter. A higher cost function J_j is accepted if the Metropolis function is greater than a random number between 0 and 1. Two applications of the technique to oceanographic problems are Barth and Wunsch (1990) and Kruger (1993). A good outline of the simulated annealing algorithm is found in Kruger (1993).

An advantage of simulated annealing is that it is independent of the structure and analytical properties of the cost function and only requires the evaluation of the cost function. Also, the method is independent of the initial guess because the algorithm enforces a randomization of the initial guess. The major disadvantage is that the stochastic nature of the algorithm requires a large amount of computer time to reach an acceptable final state. Furthermore, the reliability of the method depends on the quality of the cooling scheme, because for practical cooling schemes one cannot guarantee convergence to a global minimum (cooling schemes exist which guarantee convergence to a global minimum but in practice they are too slow).

Following Kruger, the simulated annealing required 6 parameters: the initial temperature (T_o); a vector representing the standard deviations of gaussian error to be added to the model parameters ($\boldsymbol{\sigma}_o$); the reduction factors for T_o and $\boldsymbol{\sigma}_o$ after each annealing step, dT and $d\boldsymbol{\sigma}$ respectively; the maximum number of perturbations per annealing step (N_{max}); the maximum number of acceptable perturbations required

before exiting from an annealing step. The vector $\boldsymbol{\sigma}_o$ was set to the standard deviation of the model parameters given in Table 1. To calculate the initial value of T_o, 1000 perturbations were performed by adding gaussian errors with standard deviations $\boldsymbol{\sigma}_o$ to the initial model parameters and calculating the mean change of the cost function, $\langle \Delta J \rangle$. T_o was then given by

$$T_o = -\frac{\langle \Delta J \rangle}{\ln \chi} \tag{29}$$

where χ was the probability of simulations with higher values of the cost function to be accepted. χ was set to a value of 0.90.

When running the algorithm, if N_{max} parameter simulations were performed or N_g parameter simulations were accepted, then T was reduced to $T = T\,dT$. For a given value of T, if N_{max} simulations were performed, $\boldsymbol{\sigma}$ was reduced to $\boldsymbol{\sigma} = \boldsymbol{\sigma}\,d\sigma$. The remaining simulated annealing parameters were set to $dT = 0.5$, $d\sigma = 0.75$, $N_{max} = 2500$ and $N_g = 550$. These parameters were arrived at by testing to insure the algorithm converged to the same value of the cost function independent of the initial guess of the model parameters.

On a DEC alpha 3000/400, the optimizations required approximately 60 minutes of cpu for the 3-component model and 180 minutes for the 7-component model. The factors controlling the numerical demands of simulated annealing are the complexity of the ecosystem model which was integrated many thousands of times, and the number of parameters to optimize. Simulated annealing algorithm is well suited for these optimizations because it is numerically efficient to integrate the ecosystem models and because the number of parameters to be optimized was small. More efficient algorithms are available for solving a nonlinear optimization, such as a conjugate gradient, however when the cost function is a complex surface, the algorithm has a tendency to terminate at a local minimum (Marotzke, 1992). This makes the scheme very sensitive to the choice of the initial model parameters.

To compare the performance of simulated annealing and conjugate gradient algorithm, the optimal parameters were also determined using a conjugate gradient algorithm. Only for the 3-component model did the conjugate gradient algorithm converge to an acceptable minimum, in about one third of the cpu time required by the optimization with simulated annealing. For the more complicated 4- and 7-component models, the conjugate gradient algorithm failed. This failure was attributed to the complex shape of cost function, J, caused by non-linearities in the model which lead to discontinuities in the cost function. To successfully use the conjugate gradient algorithm with these models would require optimizing the model parameters with many different initial guesses of the model parameters in an attempt to find the global minimum. Given this situation, the simulated annealing technique was the better choice. Another added benefit of simulated annealing is that it does not require information on the gradient of the cost function with respect to the

different model parameters. This reduces the coding required in implementing the algorithm, enabling one to explore several different model configurations without much additional effort.

c. Error analysis

In order for the solution of the model parameters to be complete, it must include estimates of the uncertainty in the optimal model parameters. When the errors in the observations are assumed to be normally distributed this information is obtained by analyzing the Hessian matrix (Tziperman and Thacker, 1989). The Hessian matrix, **H**, is defined as

$$\mathbf{H} = \frac{\partial^2 J}{\partial x_i \partial x_j} \qquad \text{for } i, j = 1, \ldots m. \tag{30}$$

By expanding cost function, J, in a power series about the optimal solution x^*, to the lowest order in x yields

$$J = J_{min} + \tfrac{1}{2}(x - x^*)^T \mathbf{H}(x - x^*), \tag{31}$$

where the third and higher-order terms are neglected. If the neglected terms were sufficiently small, then the uncertainties in the optimal model parameters are normally distributed with zero mean and with an error-covariance matrix defined as the inverse of the Hessian, $\mathbf{C} = \mathbf{H}^{-1}$ (Thacker, 1987). The error-covariance matrix provides information on the probability distribution of the optimal parameters. The diagonal elements of the error-covariance matrix provide a measure of the width of the distribution for the different optimal parameters. In previous studies which investigated the sensitivity of an ecosystem model to different model parameters (Fasham *et al.*, 1990; Frost, 1987), the sensitivity of the model was obtained by separately perturbing each model parameter and observing the effect on the output of the model. Such parameter sensitivity analysis is comparable to the parameter uncertainties provided by the diagonal elements of the covariance matrix. However, the approaches are inversely related; the parameter uncertainties given by the diagonal elements of the covariance matrix provide values for separately perturbing each model parameter to generate a constant change in the value of the cost function. Therefore, the smaller the parameter uncertainty, the more sensitive the model output (measured by the cost function) is to changes to that parameter. A convenient way to compare the model sensitivity to the different model parameters is to divide the parameter uncertainties by their optimal values to give their relative uncertainties.

The estimate of the model parameter uncertainties or parameter sensitivity only contain part of the information available on the sensitivity of the model to the different model parameters. The off-diagonal elements of the covariance matrix indicate the degree to which pairs of model parameters are correlated. To show the

Table 3. Summary of model optimizations with the three different ecosystem model configurations. The values of the three penalty terms of the cost function (Eq. 27) have been multiplied by two and divided by the total number of constraints ($nt + m$ + number components in the model). An acceptable Chi-squared misfit of optimal model with the constraints should produce a final cost function of approximately one (Tarantola, 1987).

Model	Comments	Number of model parameters (m)	Number of data constraints (nt)	Data misfit penalty	*A priori* parameter penalty	Steady-state penalty	Final cost function (J)	Figure number
3-component ecosystem model								
I	Reference model	11	1095	0.785	0.222	6.05E-22	1.01	4
II	Reference model with $\alpha = 0.025$	10	1095	0.84	0.229	1.02E-22	1.07	
III	Model II with constraint on microzooplankton	10	1460	1.05	0.104	1.00E-22	1.15	6
4-component ecosystem model								
IV	Reference Model	15	1460	0.8999	0.176	2.04E-04	1.09	7
V	Model IV with $\alpha = 0.025$ and constraints on the microzooplankton	14	1825	1.281	0.131	7.74E-03	1.50	8
7-component ecosystem model								
VI	Reference model	20	1095	0.851	0.077	4.71E-08	0.93	9
VII	Model VI with constraint on *f*-ration and $\alpha = 0.025$	19	1460	1.5952	0.119	2.13E-04	1.73	10

relationship between the various parameters, a correlation matrix was calculated from the error covariance matrix (Tarantola, 1987). The correlation matrix provided both the relationship between various parameters at the optimal solution and indicated the number of independent parameters which were constrained by the data used in the optimization.

In the model, the Hessian matrix was evaluated using a 3-point centered finite differencing scheme. To calculate the error-covariance matrix, the Hessian matrix was inverted using a Singular Value Decomposition (*SVD*) algorithm. The *SVD* algorithm allows one to invert a singular matrix and provide the rank and condition number of the inverted matrix.

5. Model results for Station P

The simulated annealing optimization was applied to the 3-, 4- and 7-component ecosystem model configurations to determine optimal model parameters at Station P. Table 3 summarizes the different model optimizations performed in this study. For the three model configurations, the reference run refers to an optimization of the model parameters where the output of the ecosystem model was constrained by the nitrate, phytoplankton, mesozooplankton (only for 4-component ecosystem model) concentrations in the mixed layer, the net phytoplankton productivity (*NPP*) from

Table 4. Model I optimal parameters with the estimated one standard deviation uncertainty (same units as given in Table 1).

Model	Parameter	Standard deviation uncertainty	Relative uncertainty
K_1	1.368	3.009	2.200
μ_1	0.0002	0.006	30.0
θ	0.123	0.048	0.390
K_3	1.315	0.450	0.342
g	0.952	0.067	0.070
γ_2	0.500	0.001	0.002
μ_5	0.015	0.002	0.133
PAR	0.500	—	—
α	0.005	0.001	0.20
K_w	0.040	—	—
K_c	0.060	—	—
m	2.064	0.149	0.072
γ_5	0.518	0.018	0.035
γ_4	0.484	0.055	0.114

the mixed layer and by *a priori* model parameters. To these reference runs, additional constraints are introduced to the model to improve the model output and assess their effect on the optimal model parameters.

a. 3-component ecosystem model

The optimization of the reference run (model I) successfully reproduces the observed nitrate, phytoplankton and *NPP* observations (Fig. 4). The model also produces very high concentrations of zooplankton in the mixed layer. Before dealing with the high zooplankton concentrations, it would be instructive to first discuss the error-covariance matrix of the optimal model parameters.

The error-covariance matrix of the optimal model parameters provides insight into the behavior of the ecosystem model. Shown in Table 4 are the calculated model parameters along with their estimated (one standard deviation) uncertainty determined from the diagonal elements of the error-covariance matrix. All optimal model parameters appear reasonable with the exception of μ_1, μ_5 and α parameters which are too small. The calculated model parameter uncertainties indicate that the parameters, g, γ_2, γ_5 and m are the parameters best determined by the optimization and hence that the model output is most sensitive to these parameters. The small uncertainities in some of the parameters controlling the zooplankton biomass indicate that these parameters are well-defined by data constraints without explicit constraints on the zooplankton concentrations. The high model sensitivity to m is the consequence of requiring the model nitrate concentrations in the mixed layer to approximate the observations.

Table 5. The correlation coefficients between the optimal parameters of model I.

	Model Parameters										
	K_1	μ_1	θ	K_3	g	γ_2	μ_5	α	m	γ_5	γ_4
K_1	**1.00**	**−0.96**	**0.95**	−0.38	0.37	0.28	−0.52	**−0.97**	0.60	0.45	−0.13
μ_1	**−0.96**	**1.00**	**−0.83**	0.12	−0.38	−0.39	0.71	**0.88**	−0.54	−0.41	0.10
θ	**0.95**	**−0.83**	**1.00**	−0.63	0.32	0.14	−0.25	**−0.99**	0.58	0.44	−0.15
K_3	−0.38	0.12	−0.63	**1.00**	0.11	0.31	−0.55	0.53	−0.42	−0.26	0.04
g	0.37	−0.38	0.32	0.11	**1.00**	0.12	−0.21	−0.32	0.27	0.18	−0.03
γ_2	0.28	−0.39	0.14	0.31	0.12	**1.00**	−0.53	−0.21	−0.01	0.20	0.19
μ_5	−0.52	0.71	−0.25	−0.55	−0.21	−0.53	**1.00**	0.37	−0.11	−0.13	0.15
α	**−0.97**	**0.88**	**−0.99**	0.53	−0.32	−0.21	0.37	**1.00**	−0.49	−0.41	0.18
m	0.60	−0.54	0.58	−0.42	0.27	−0.01	−0.11	−0.49	**1.00**	0.49	0.11
γ_5	0.45	−0.41	0.44	−0.26	0.18	0.20	−0.13	−0.41	0.49	**1.00**	0.13
γ_4	−0.13	0.10	−0.15	0.04	−0.03	0.19	0.15	0.18	0.11	0.13	**1.00**

For model I, the inversion of the Hessian is ill-conditioned (condition number = 10^6) indicating that a number of the model parameters are highly correlated. The correlation matrix calculated from the error-covariance matrix gives the correlation coefficients between all pairs of optimal model parameters for model I (Table 5). This table reveals that the parameters separate into one set of highly correlated parameters ($|r| > 0.8$) and 7 independent parameters. The formulated optimization problem is only able to uniquely determine 8 independent parameters. The set of highly correlated parameters, μ_1, K_1, θ and α are systematically related and therefore the solution determined for these parameters is not unique. For example, fixing α = 0.025 (W m^{-2} d)$^{-1}$, the optimization routine (model II) produces model output that is nearly identical to the output from the reference model as evident in the similar values of the final cost function (Table 3).

The output of model I and model II produces high concentrations of zooplankton. Although there are very limited data on the microzooplankton concentrations at Station P (Boyd *et al.,* 1995), both models predicted considerably greater concentrations than expected. To investigate the effect of a lower zooplankton concentration on the model, an artificial constraint on the zooplankton concentration is employed (model III). With this added constraint, the model still produces a good fit with the data (Fig. 7). The model generates a small increase in phytoplankton concentrations from 0.1 to 0.3 μmol kg^{-1} in the spring and a slightly reduced *NPP* in spring (Fig. 7) as compared to the reference model (Fig. 4). The presence of the weak spring phytoplankton bloom is caused by the imbalance between the rapidly growing phytoplankton and the grazing of phytoplankton by the zooplankton. The imbalance is initiated by presence of a feeding threshold in the zooplankton grazing which turns-off zooplankton grazing until the threshold concentration is exceeded. Once the phytoplankton concentration exceeds this threshold the imbalance is quickly restored as the zooplankton graze down the phytoplankton. For this model configu-

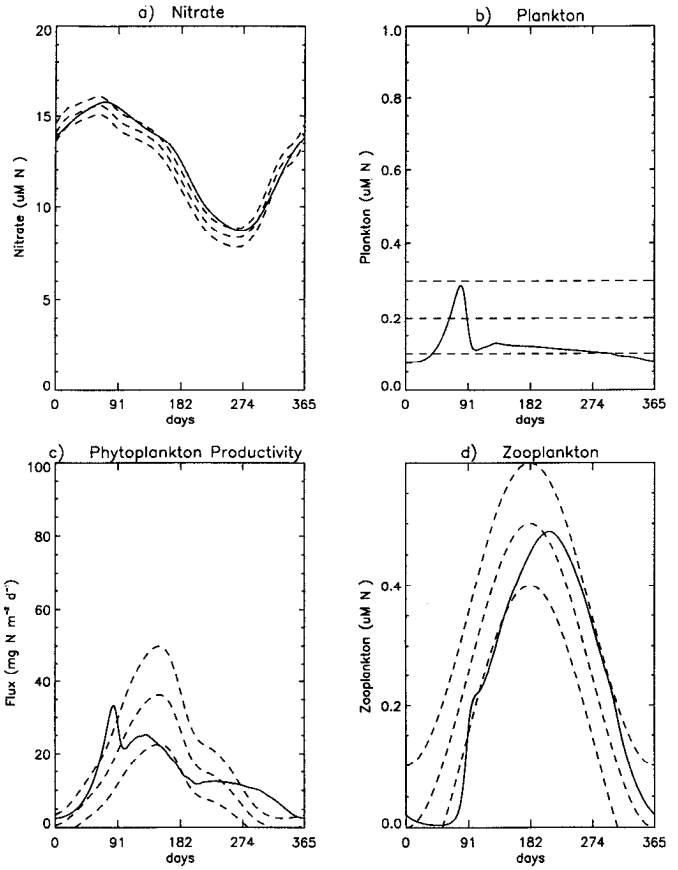

Figure 7. Model III (3-component ecosystem model) as Figure 5.

rations, the feeding threshold parameter is necessary to stabilize the model, and without this parameter the model displays very erratic behavior.

Optimal parameters from model III along with their estimated uncertainties are given in Table 6. The constraint on the zooplankton concentrations cause K_3 to decrease by 1 μM to 0.43 μM, g to increase by 13% to 1.07 d^{-1} and μ5 to increase by 0.03 d^{-1} to 0.047 d^{-1} from that of model II. The other model parameters are not significantly affected by including the zooplankton constraint. With the exception of the mortality rate of zooplankton, μ_5, the parameters displaying the largest uncertainty in model I did not experience a reduction in uncertainty in model III. This indicates that the added zooplankton constraint does not further constrain these parameters. However, the zooplankton constraint is important to increasing the value of μ_5 and reducing its relative uncertainty. With the added zooplankton constraint, the correlation matrix does not significantly change from the correlation

Table 6. Model III optimal parameters with the estimated one standard deviation uncertainty (same units as given in Table 1).

Model	Parameter	Standard deviation uncertainty	Relative uncertainty
K_1	4.786	4.739	0.990
μ_1	0.035	0.013	0.371
θ	0.074	0.034	0.460
K_3	0.431	0.093	0.215
g	1.075	0.085	0.080
γ_2	0.504	0.001	0.002
μ_5	0.047	0.002	0.043
PAR	0.500	—	—
α	0.025	—	—
K_w	0.040	—	—
K_c	0.060	—	—
m	2.312	0.203	0.088
γ_5	0.527	0.021	0.040
γ_4	0.570	0.076	0.133

matrix for model I (Table 5); still only 8 independent parameters are resolved by the optimization problem.

By only relying on the nitrate, phytoplankton and *NPP* data, the model does not produce acceptable zooplankton concentrations. Tests with this model configuration did show that the zooplankton concentration is sensitive to only a few model parameters and that small changes to these parameters produce large changes in the zooplankton concentration. Modeling work by McAllister (1969) also exhibited large fluctuations in the zooplankton biomass when the zooplankton growth and mortality terms were changed by small amounts.

b. 4-component ecosystem model

The 4-component model configuration was formulated in an attempt to produce more acceptable microzooplankton concentrations than the 3-component configuration. The addition of another trophic level to the model enables one to include the mesozooplankton data but increases the model complexity. The 4-component reference model (model IV) is successful at reproducing the nitrate, phytoplankton and *NPP* observations (Fig. 6), however, this model predicts higher microzooplankton concentrations and a peak in the mesozooplankton concentrations that occurs later in the season than observed.

The optimal model parameters for this model, along with their calculated uncertainties, are given in Table 7. Both the 3-component and the 4-component models predicted similar values for diffusion (m) with small uncertainty which indicated that this parameter is not sensitive to the formulation of the ecosystem model. The uncertainties of the 4-component model parameters are all greater than the uncer-

Table 7. Model IV optimal parameters with the estimated one standard deviation uncertainty (same units as given in Table 1).

Model	Parameter	Standard deviation uncertainty	Relative uncertainty
K_1	2.246	3.665	1.627
μ_1	0.0002	0.010	50.0
θ	0.121	0.032	0.264
K_3	1.131	0.682	0.603
g	0.133	0.069	0.519
γ_2	0.470	0.133	0.283
μ_5'	0.009	0.0001	0.011
PAR	0.500	—	—
α	0.010	0.001	0.100
K_w	0.040	—	—
K_c	0.060	—	—
m	2.143	0.153	0.071
γ_5'	0.554	0.028	0.051
g'	0.068	0.011	0.162
K_3'	0.939	0.087	0.093
γ_5	0.604	0.021	0.035
γ_2'	0.189	0.029	0.153
γ_4'	0.345	0.083	0.240

tainties for corresponding parameter of the 3-component model. The increases in the 4-component model parameter uncertainties show that by adding the mesozooplankton component to the 3-component model, the model complexity increases more than the constraints.

Like the 3-component model, the correlation matrix calculated from the error-covariance matrix of model IV reveals that many of the parameters are highly correlated (Table 8). The model parameters separate into 3 sets of highly correlated parameters ($|r| > 0.8$) and 7 independent parameters. The 3 sets of highly correlated parameters are (1) K_1, μ_1, θ, $\gamma 2$ and α, (2) K_3 and g and (3) g' and γ_2'. The optimization problem determines only 10 independent parameters; the optimal parameters are not a unique solution. The 4-component model determines 2 more independent parameters than the 3-component model but requires 4 additional parameters. By setting $\alpha = 0.025$ $(\mathrm{W\,m^{-2}\,d})^{-1}$, the optimal parameters produce model output that does not change nitrate, phytoplankton and *NPP* and only slightly reduces the micro and mesozooplankton concentrations.

By imposing an artificial microzooplankton constraint on the 4-component ecosystem model (model V), along with $\alpha = 0.025$ $(\mathrm{W\,m^{-2}\,d})^{-1}$, the optimal parameters produce the results shown in Figure 8. The model produces a small peak in the phytoplankton concentrations in the spring, and underestimates the *NPP* in summer. Like the 3-component ecosystem model configuration, the weak spring phytoplank-

Table 8. Correlation coefficients between the optimal parameters of model IV.

	Model Parameters														
	K_1	μ_1	θ	K_3	g	γ_2	μ_5'	α	m	γ_5	g'	K_3'	γ_5'	γ_2'	γ_4'
K_1	**1.00**	**−0.98**	**0.99**	0.05	0.00	**0.93**	−0.77	**−0.99**	−0.27	0.64	0.66	0.29	−0.01	−0.46	−0.01
μ_1	**−0.98**	**1.00**	**−0.96**	−0.06	0.00	**−0.94**	0.72	**0.97**	0.09	−0.67	−0.68	−0.28	0.00	0.49	0.01
θ	**0.99**	**−0.96**	**1.00**	−0.02	−0.06	**0.92**	−0.76	**−0.99**	−0.33	0.63	0.66	0.29	−0.01	−0.46	−0.02
K_3	0.05	−0.06	−0.02	**1.00**	**0.99**	0.04	−0.15	0.03	0.02	0.03	0.00	0.00	0.00	−0.02	0.00
g	0.00	0.00	−0.06	**0.99**	**1.00**	−0.06	−0.18	0.07	0.00	−0.03	−0.13	−0.03	0.00	0.13	0.00
γ_2	**0.93**	**−0.94**	**0.92**	0.04	−0.06	**1.00**	−0.51	**−0.91**	−0.15	0.67	0.87	0.24	−0.01	−0.74	−0.01
μ_5'	−0.77	0.72	−0.76	−0.15	−0.18	−0.52	**1.00**	0.78	0.27	−0.41	−0.06	−0.19	−0.01	−0.17	0.00
α	**−0.99**	**0.97**	**−0.99**	0.03	0.07	**−0.91**	0.78	**1.00**	0.25	−0.64	−0.62	−0.26	0.00	0.41	0.01
m	−0.27	0.09	−0.33	0.02	0.00	−0.15	0.27	0.25	**1.00**	0.03	−0.12	−0.04	0.02	0.07	0.03
γ_5	0.64	−0.67	0.63	0.03	−0.03	0.67	−0.41	−0.64	0.03	**1.00**	0.53	0.16	0.00	−0.42	0.01
g'	0.66	−0.68	0.66	0.00	−0.13	0.87	−0.06	−0.62	−0.12	0.53	**1.00**	0.33	−0.01	**−0.96**	−0.01
K_3'	0.29	−0.28	0.29	0.00	−0.03	0.24	−0.19	−0.26	−0.04	0.16	0.33	**1.00**	0.00	−0.12	−0.01
γ_5'	−0.01	0.00	−0.01	0.00	0.00	−0.01	−0.01	0.00	0.02	0.00	−0.01	0.00	**1.00**	0.01	0.00
γ_2'	−0.46	0.49	−0.46	−0.02	0.13	−0.74	−0.17	0.41	0.07	−0.42	**−0.96**	−0.12	0.01	**1.00**	0.00
γ_4'	−0.01	0.01	−0.02	0.00	0.00	−0.01	0.00	0.01	0.03	0.01	−0.01	−0.01	0.00	0.00	**1.00**

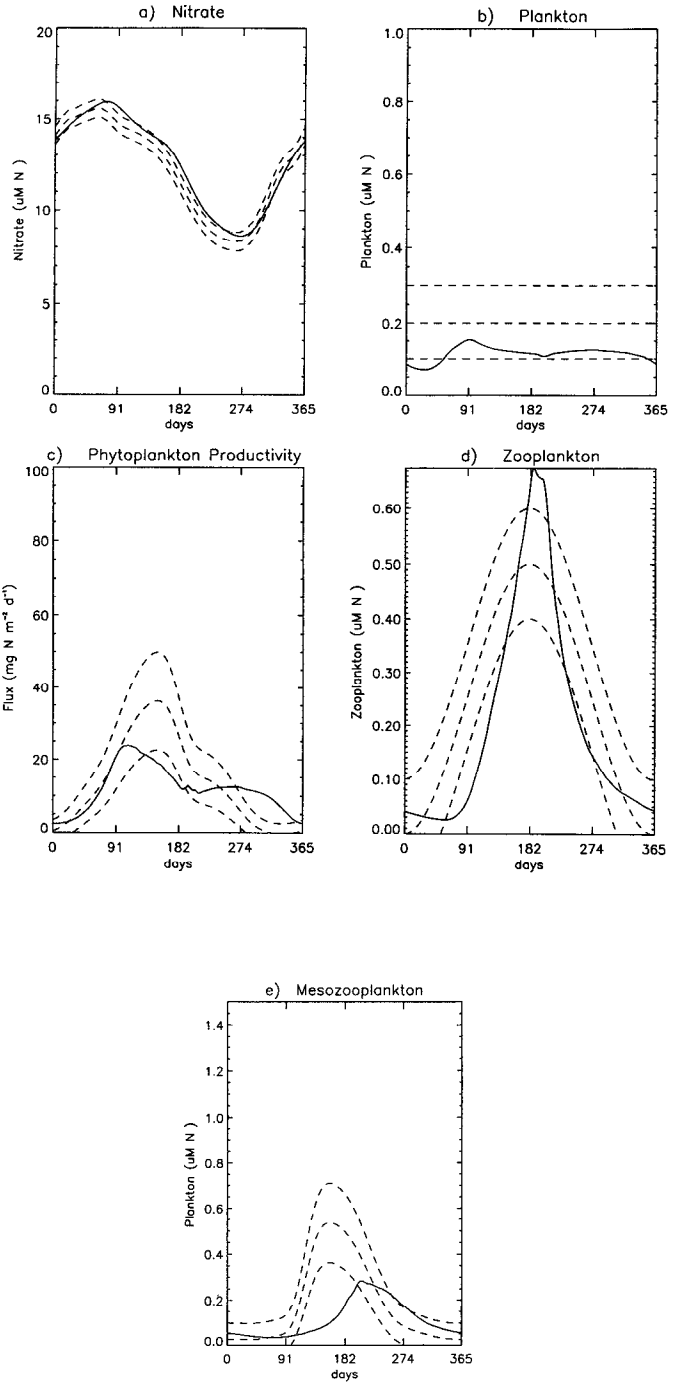

Figure 8. Model V (4-component ecosystem model) as for Figure 7.

Table 9. Model V optimal parameters with the estimated one standard deviation uncertainty (same units as given in Table 1).

Model	Parameter	Standard deviation uncertainty	Relative uncertainty
K_1	5.148	5.796	1.126
μ_1	0.051	0.005	0.097
θ	0.107	0.028	0.266
K_3	0.283	0.543	1.919
g	0.1450	1.652	1.140
γ_2	0.191	0.208	1.091
μ_5'	0.010	0.000	0.045
PAR	1.000	—	—
α	0.025	—	—
K_w	0.040	—	—
K_c	0.060	—	—
m	2.421	0.286	0.118
γ_5	0.533	0.057	0.108
g'	0.154	0.002	0.015
K_3'	1.095	0.862	0.787
γ_5'	0.607	0.026	0.043
γ_2'	0.295	0.157	0.532
γ_4'	0.349	0.104	0.297

ton bloom is caused by the presence of the feeding threshold parameter in microzooplankton grazing.

The optimal model parameters have low zooplankton efficiency (γ_2) and a low grazing rate of mesozooplankton (g') (Table 9). Compared to the 3-component model (model III), model V shows an increase in the values of K_1 and θ by 3.0 and 0.05 respectively and a decrease in the values of K_3 and γ_2 by 0.2 and 0.35 respectively. The parameters of model V have larger uncertainties than the corresponding parameters of model III. The error-covariance matrix of model V parameters still shows that only 10 independent parameters are determined.

To produce acceptable concentrations of micro- and mesozooplankton, the computed optimal parameters are not realistic for parameters that describe the growth rate of micro- and mesozooplankton. This indicates that the formulation of this ecosystem model is inconsistent with the data, and the model requires modification to resolve this inconsistency (i.e. temperature-dependent zooplankton grazing rates or non-linear mortality rate for mesozooplankton).

c. 7-component ecosystem model

The optimization of the 7-component reference model (model VI) produced model output that resembled the data and produced a reasonable zooplankton concentration (Fig. 9). The lack of the spring phytoplankton bloom is attributed to

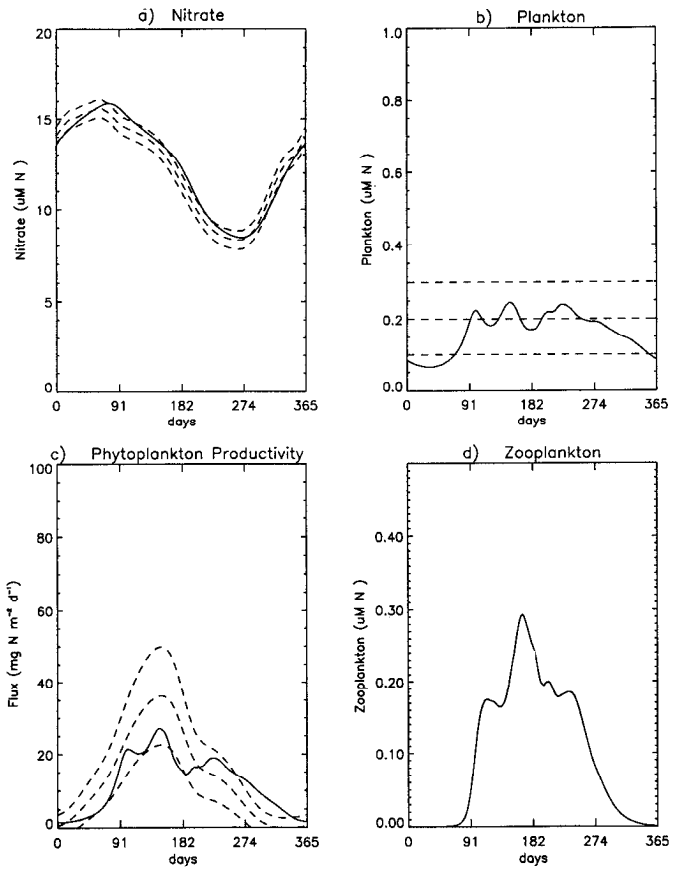

Figure 9. Reference of the 7-component ecosystem model (model VI) for the mixed layer (a) nitrate concentration, (b) phytoplankton concentration, (c) net phytoplankton productivity, (d) microzooplankton concentration, (e) f-ratio, (f) bacteria concentration, (g) ammonium concentration. The solid lines refer to the model and the three dashed lines are the data and the data with ± one standard deviations uncertainty.

absence of a feeding threshold in the grazing of phytoplankton by zooplankton which enables the zooplankton to more closely track the phytoplankton population than the previous models. However, the model's *f*-ratio in the summer is 0.9 (*f*-ratio is the ratio of new production to total production), much greater than the measured summer *f*-ratio of approximately 0.5 made by Wheeler and Kokkinakis (1990) at Station P.

The optimal parameters determined from the reference model produce a value for diffusion (m) similar to the previous 3- and 4-component models (Table 10). The uncertainties in the parameters of the 7-component model that are comparable to the 3- and 4-component model are all greater than the correspnding parameters from the 3- and 4-components models (models I and IV). The model parameters

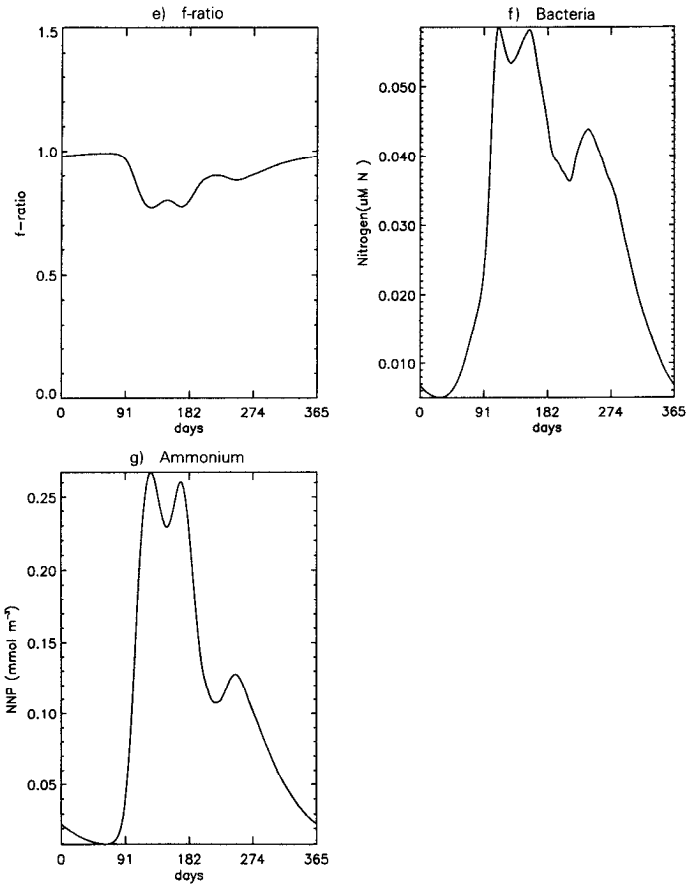

Figure 9. (Continued)

m,γ_1, μ_2, γ_3 and γ_4 have the smallest relative uncertainties showing that the model output is most sensitive to changes in these parameters.

The inversion of the Hessian matrix, required to determine the error covariance matrix for model VI parameters, has a condition number that is 2 orders of magnitude greater than the 3-component model, indicating that the problem is more ill-conditioned than the 3-component model and that many parameters are not independently resolved. The correlation between the various parameters is more complicated than in the previous 3- and 4-component models (Table 11). The parameters separated into one group of parameters that exhibited high correlations with each other and 8 independently resolved parameters. The lack of a distinct pattern to the highly correlated parameters demonstrates that the model was more non-linear than the previous models. The larger uncertainty in the optimal parameters and the large number of highly correlated parameters indicated that the model constraints are insufficient to properly constrain many of the model parameters.

Table 10. Model VI optimal parameters with the estimated one standard deviation uncertainty (same units as given in Table 1).

Model	Parameters	Standard deviation uncertainty	Relative uncertainty
PAR	0.50	—	—
K_w	0.040	—	—
K_c	0.060	—	—
m	2.144	0.240	0.112
K_1	1.190	5.429	4.562
μ_1	0.0002	0.037	185.0
γ_1	0.050	0.005	0.10
Ψ	1.500	—	—
g	1.410	1.409	1.000
γ_2	0.596	0.498	0.836
α	0.009	0.011	1.222
μ_2	0.107	0.078	0.730
μ_5	0.052	0.002	0.038
K_3	0.569	0.757	1.330
γ_4	0.341	0.021	0.062
γ_3	0.746	0.012	0.016
V_b	2.094	1.776	0.848
μ_3	0.052	0.056	1.08
K_4	0.418	1.078	2.580
η	0.615	0.258	0.419
μ_4	0.053	0.178	3.358
w_s	3.495	16.903	4.834
p_1	0.136	0.333	2.445
p_2	0.438	0.159	0.363

To reconcile the model with the observed *f*-ratios, the model was run with $\alpha = 0.025$ (W m^{-2} d)$^{-1}$ and a constraint on the *f*-ratio (model VII). With this constraint, the fit to the other constraints is degraded, $J = 1.73$ (Table 3). The optimal parameters produced a model output which has lower phytoplankton concentrations, reduced *NPP* in the summer and decreased zooplankton concentrations (Fig. 10) from that of model VI. The average *f*-ratio for the model is ≈ 0.5. The addition of the *f*-ratio constraint significantly changes the values of the optimal parameters and their corresponding uncertainties (Table 12). The constraint reduced the sensitivity of the model output of m, γ_1, μ_2, γ_3 and γ_4 but made the model extremely sensitive to K_4, the half saturation constant for bacterial uptake. Model VII output is also much more sensitive to zooplankton preference for phytoplankton grazing, ρ_1.

Only limited comparison of the modeled ammonium and bacteria concentrations can be made with observations at Station P. Ammonium measurements of Wheeler and Kokkinakis (1990) gave summer ammonium concentrations of 0.2 μM N which are consistent with the model. The bacterial abundance measurements of Kirchman

Table 11. Correlation coefficients between the optimal parameters of model VI.

	Model Parameters																			
	m	K_1	μ_1	γ_1	g	γ_2	α	μ_2	μ_5	K_3	γ_4	γ_3	V_b	μ_3	K_4	η	μ_4	w_s	p_1	p_2
m	**1.00**	0.42	−0.07	−0.62	−0.24	−0.13	0.20	0.74	0.36	−0.30	−0.46	0.07	−0.21	0.09	0.34	−0.31	−0.42	−0.36	0.29	0.25
K_1	0.42	**1.00**	**0.86**	**−0.92**	0.12	**0.81**	**0.97**	0.02	−0.37	0.01	−0.59	0.77	0.37	**0.93**	−0.63	−0.27	0.58	0.64	−0.69	−0.67
μ_1	−0.07	**0.86**	**1.00**	−0.65	0.25	**0.99**	**0.96**	−0.44	−0.68	0.18	−0.38	**0.81**	0.53	**0.98**	**−0.91**	−0.13	**0.92**	**0.94**	**−0.95**	**−0.91**
γ_1	−0.62	**−0.92**	−0.65	**1.00**	0.01	−0.61	**−0.82**	−0.23	0.21	0.06	0.60	−0.60	−0.14	−0.75	0.35	0.30	−0.31	−0.37	0.41	0.42
g	−0.24	0.12	0.25	0.01	**1.00**	0.29	0.19	−0.65	−0.25	**0.96**	0.12	0.46	0.17	0.26	−0.30	−0.05	0.35	0.33	−0.42	−0.44
γ_2	−0.13	**0.81**	**0.99**	−0.61	0.29	**1.00**	**0.93**	−0.52	−0.73	0.25	−0.33	0.79	0.55	**0.96**	**−0.92**	−0.10	**0.93**	**0.95**	**−0.94**	**−0.90**
α	0.20	**0.97**	**0.96**	**−0.82**	0.19	**0.93**	**1.00**	−0.20	−0.54	0.09	−0.51	**0.82**	0.47	**0.99**	−0.79	−0.21	0.77	**0.81**	**−0.84**	**−0.81**
μ_2	0.74	0.02	−0.44	−0.23	−0.65	−0.52	−0.20	**1.00**	0.65	−0.71	−0.29	−0.37	−0.32	−0.31	0.61	−0.11	−0.72	−0.67	0.64	0.62
μ_5	0.36	−0.37	−0.68	0.21	−0.25	−0.73	−0.54	0.65	**1.00**	−0.30	0.11	−0.46	−0.34	−0.58	0.71	0.18	−0.77	−0.76	0.70	0.66
K_3	−0.30	0.01	0.18	0.06	0.96	0.25	0.09	−0.71	−0.30	**1.00**	0.20	0.36	0.10	0.17	−0.23	−0.03	0.30	0.27	−0.32	−0.36
γ_4	−0.46	−0.59	−0.38	0.60	0.12	−0.33	−0.51	−0.29	0.11	0.20	**1.00**	−0.35	−0.13	−0.46	0.21	0.21	−0.15	−0.20	0.23	0.23
γ_3	0.07	0.77	**0.81**	−0.60	0.46	0.79	0.82	−0.37	−0.46	0.36	−0.35	**1.00**	0.42	**0.84**	−0.71	−0.12	.71	0.73	−0.79	−0.78
V_b	−0.21	0.37	0.53	−0.14	0.17	0.55	0.47	−0.32	−0.34	0.10	−0.13	0.42	**1.00**	0.52	−0.53	0.02	0.57	0.57	−0.57	−0.47
μ_3	0.09	**0.93**	**0.98**	−0.75	0.26	**0.96**	**0.99**	−0.31	−0.58	0.17	−0.46	**0.84**	0.52	**1.00**	**−0.85**	−0.15	**0.83**	**0.87**	**−0.90**	**−0.85**
K_4	0.34	−0.63	**−0.91**	0.35	−0.30	**−0.92**	−0.79	0.61	0.71	−0.23	0.21	−0.71	−0.53	**−0.85**	**1.00**	0.01	**−0.96**	**−0.96**	**0.95**	**0.87**
η	−0.31	−0.27	−0.13	0.30	−0.05	−0.10	−0.21	−0.11	0.18	−0.03	0.21	−0.12	0.02	−0.15	0.01	**1.00**	0.01	−0.01	0.07	0.07
μ_4	−0.42	0.58	0.92	−0.31	0.35	**0.93**	0.77	−0.72	−0.77	0.30	−0.15	0.71	0.57	**0.83**	**−0.96**	0.01	**1.00**	**1.00**	**−0.98**	**−0.92**
w_s	−0.36	0.64	**0.94**	−0.37	0.33	**0.95**	**0.81**	−0.67	−0.76	0.27	−0.20	0.73	0.57	**0.87**	**−0.96**	−0.01	**1.00**	**1.00**	**−0.98**	**−0.92**
p_1	0.29	−0.69	**−0.95**	0.41	−0.42	**−0.94**	**−0.84**	0.64	0.70	−0.32	0.23	−0.79	−0.57	**−0.90**	**0.95**	0.07	**−0.98**	**−0.98**	**1.00**	**0.93**
p_2	0.25	−0.67	**−0.91**	0.42	−0.44	**−0.90**	**−0.81**	0.62	0.66	−0.36	0.23	−0.78	−0.47	**−0.85**	**0.87**	0.07	**−0.92**	**−0.92**	**0.93**	**1.00**

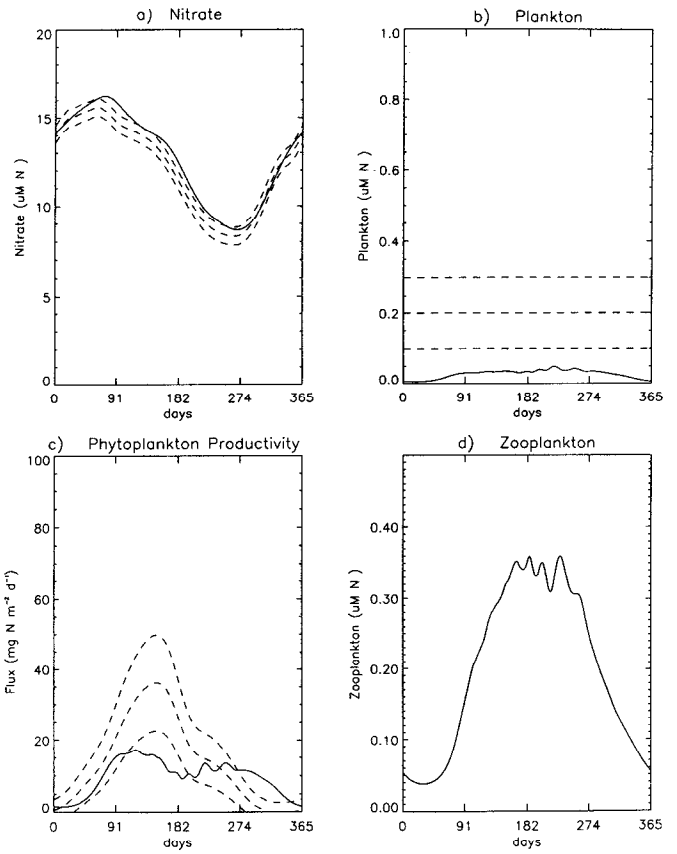

Figure 10. Model VII (7-component ecosystem model) as Figure 9.

et al. (1990) and Simon *et al.* (1992) gave an estimated summer bacterial biomass of 0.3 μM N which is considerably greater than the summer value of the model. To validate this model clearly requires more data on the ammonium and bacteria concentrations.

6. Discussion and conclusion

Parameter optimization of an ecosystem model provides a direct technique for determining model parameters in a way that produces results that are consistent with the observed data. The optimization problem can be formulated in a very general manner and is easily modified to include additional data constraints as well as constraints on the model parameters provided by direct measurements. The automation of the process for determining the model parameters enables one to test a variety of ecosystem model configurations to determine their suitability for use with

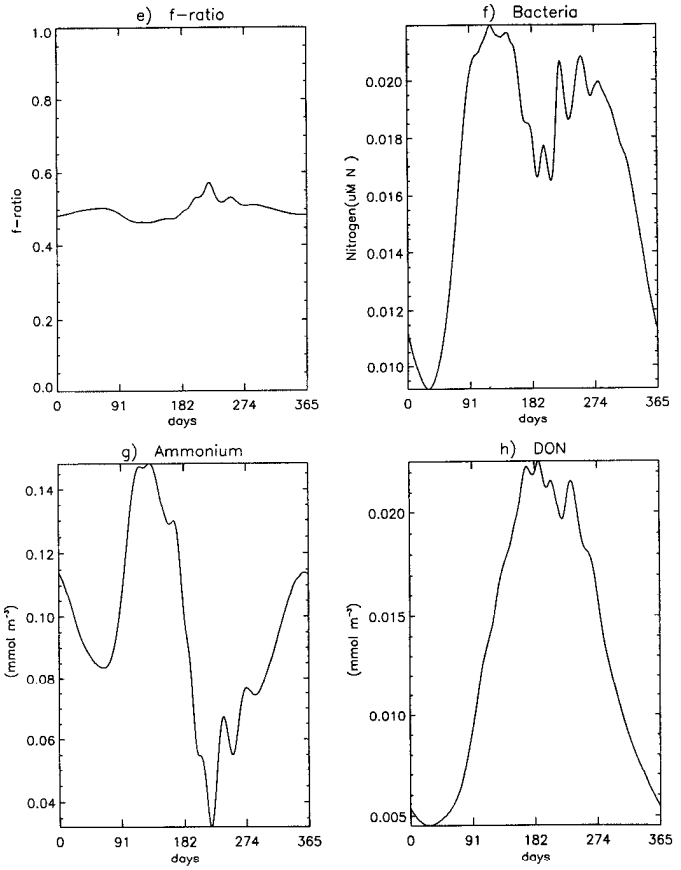

Figure 10. (Continued)

the available data. The calculation of the error covariance matrix of the optimal parameters provides a way of evaluating the sensitivity of the model output to the model parameters and assessing the correlations between the various parameters. This determines the number of independent parameters in the ecosystem model.

Optimal parameters of an ecosystem model were determined by simulated annealing. The limiting factor in applying a stochastic optimization scheme like simulated annealing is the computational cost. However, in these optimizations the limited number of unknowns and the simplicity of the ecosystem models means that the computational requirements are not a significant barrier to using simulated annealing. Furthermore, for these optimizations a fast annealing schedule could be used ($dT = 0.5$) which significantly improves the efficiency of the algorithm. This made simulated annealing ideally suited for these optimizations. Optimizations with simulated annealing were robust and effective at determining the optimal parameters for three ecosystem model configurations while the conjugate gradient algo-

Table 12. Model VII optimal parameters with the one standard deviation uncertainty (same units as given in Table 1).

Model	Parameters	Standard deviation uncertainty	Relative uncertainty
PAR	0.50	—	—
K_w	0.040	—	—
K_c	0.060	—	—
m	2.880	0.405	0.141
K_1	0.028	0.053	1.892
μ_1	0.083	0.060	0.723
γ_1	0.056	0.007	0.125
Ψ	1.500	—	—
g	1.155	1.497	1.295
γ_2	0.584	0.197	0.337
α	0.025	—	—
μ_2	0.062	0.013	0.210
μ_5	0.056	0.013	0.232
K_3	0.313	0.681	2.176
γ_4	0.332	0.050	0.151
γ_3	0.767	0.044	0.057
V_b	2.323	0.939	0.404
μ_3	0.064	0.034	0.531
K_4	0.118	0.0001	0.00001
η	0.508	0.999	1.967
μ_4	0.055	0.046	0.836
w_s	0.001	2.183	2.183
p_1	0.435	0.083	0.144
p_2	0.476	0.207	0.434

rithm failed on the more complex and nonlinear 4- and 7-component ecosystem models. An added benefit of simulating annealing over the conjugate gradient method is that it only needs to evaluate the cost function and not the gradient of the cost function. Such a feature is particularly useful when considering different model configurations and different model parameterizations.

At Station P, simulated annealing was used to optimize a 3-, 4- and 7-component ecosystem model configuration. The models were constrained by nitrate, phytoplankton, mesozooplankton and *NPP* data and by *a priori* values of the model parameters.

The 3-component ecosystem model is capable of reproducing the observed data. The model requires artificial data to produce reasonable zooplankton concentrations but the inclusion of this information does not greatly alter the model fit with other observations. The 4-component ecosystem configuration, which had the additional mesozooplankton component, failed to produce acceptable microzooplankton concentrations without an additional constraint on the microzooplankton concentrations. This ecosystem configuration cannot produce reasonable microzooplankton

concentrations without having some unrealistic parameters for the growth rate and mortality rate of microzooplankton and mesozooplankton. This inconsistency indicates that the model parameterization is inconsistent with the observations and requires modifications. Both, the 3- and 4-component configurations require a feeding threshold for the grazing of phytoplankton by zooplankton to stabilize these models. This threshold level allows the development of small spring blooms of phytoplankton in these models.

The 7-component ecosystem configuration did not require additional constraints on the microzooplankton to produce reasonable values and it lacks the small spring phytoplankton bloom that is produced by the 3- and 4-component models. The 7-component configuration produced no spring bloom because the model had no feeding threshold for phytoplankton grazing allowing the zooplankton growth rate to more closely follow the phytoplankton growth rate. The 7-component model required a constraint on the *f*-ratio to produce acceptable values for the *f*-ratio. Furthermore, the lack of relevant data, such as ammonium and bacteria concentrations make it difficult to validate the model. The analysis of the optimal model parameters shows a large number of highly correlated parameters with less than half of the parameters being independently determined.

The optimizations with the three different ecosystem configurations show that the available data place significant limitations on the necessary complexity required in the ecosystem model. It also reveals shortcomings in the model formulation. For three ecosystem configurations, the error-covariance matrices of the optimal model parameters show that the constraints on the models determine 10 or less independent parameters. This number is always less than the number of unknown model parameters indicating that optimal solutions are not unique. The parameter optimizations of the different ecosystem configurations reveal that the 3-component configuration is an adequate model for explaining the data at Station P. Even with this simple configuration, several model parameters cannot be resolved by the optimization scheme, and an artificial constraint on the microzooplankton concentrations was required to produce acceptable values. Measurements of microzooplankton at Station P are necessary to validate this model. To justify a more complicated ecosystem model, like the 7-component configuration, additional measurements are required. It would be extremely useful if more measurements on the *f*-ratio and the ammonium and bacteria concentrations could be obtained since Azam *et al.* (1983) suggests that the microbial loop plays an important role in the plankton dynamics in the northeast Pacific Ocean. Such measurements are essential to validate the 7-component ecosystem model.

Acknowledgments. This work was carried out with the support of the Office of Naval Research grant N00014-92-J-1775. Additional support for this research was provided by PERD grant 48105.

REFERENCES

Anderson, G. C., R. K. Lam, B. C. Booth and J. M. Glass. 1977. A description and numerical analysis of the factors affecting the processes of production in the Gulf of Alaska NOVAA, 03-5-022067, 477–798.

Azam, F., T. Fenchel, J. G. Field, J. S. Gray, L. A. Meyer-Reil and F. Thingstad. 1983. The ecological role of water-column microbes in the sea. Mar. Ecol. Prog. Ser., *10,* 257–263.

Baker, K. S. and R. Frouin. 1987. Relation between photosynthetically available radiation and total insolation at the ocean surface under clear skies. Limnol. Oceanogr., *32,* 1370–1377.

Barth, N. and C. Wunsch. 1990. Oceanographic experiment design by simulated annealing. J. Phys. Oceanogr., *20,* 1249–1263.

Boyd, P. W., S. Strom, F. Whitney, S. Doherty, M. Wen, P. J. Harrison and C. S. Wong. 1995. The northeast subarctic Pacific in winter: 1 Biological standing stocks. Marine Ecol. Progr. Ser. (in press).

Brock, T. D. 1981. Calculating solar radiation for ecological studies. Ecol. Model., *14,* 1–19.

Dobson, F. and S. Smith. 1985. Estimation of solar radiation at sea, *in* The Ocean Surface, Y. Toba *et al.,* eds., D. Reidel Publishing, New York, 525–533.

Eppley, R. W. 1972. Temperature and phytoplankton growth in the sea. Fish. Bull. U.S., *70,* 1063–1085.

Evans, G. T. and S. J. Parslow. 1985. A model of annual plankton cycles. Biol. Oceanogr., *3,* 327–347.

Fasham, M. J. R., H. W. Ducklow and S. M. McKelvie. 1990. A nitrogen-based model of plankton dynamics in the oceanic mixed layer. J. Mar. Res., *48,* 591–639.

Frost, B. 1987. Grazing control of phytoplankton stock in the open subarctic Pacific Ocean: a model assessing the role of mesozooplankton, particularly the large calanoid copepods *Neccalanus spp.* Mar. Ecol. Prog. Ser., *39,* 49–68.

—— 1991. The role of grazing in nutrient-rich areas of the open sea. Limnol. Oceanogr., *36,* 1616–1630.

Fulton, J. D. 1983. Seasonal and annual variations of net zooplankton at Ocean Station P, 1956–1980. Can. Data Rep. Fish. Aquat. Sci., *374.*

Jackson, G. A. and P. Eldridge. 1992. Food web analysis of a plankton system off Southern California. Prog. Oceanogr., *30,* 223–251.

Joos, F., J. L. Sarmiento and U. Siegenthaler. 1991. Estimates of the effect of Southern Ocean iron fertilization on atmospheric CO_2 concentrations. Nature, *349,* 772–775.

Kirchman, D. L., R. G. Keil and P. A. Wheeler. 1990. Carbon limitation of ammonium uptake by heterotrophic bacteria in the subarctic Pacific. Limnol. Oceanogr., *35,* 1258–1266.

Kirkpatrick, S., C. D. Gelatt and M. P. Vecchi. 1983. Optimization by simulated annealing. Science, *220,* 671–680.

Krüger, J. 1993. Simulated annealing: A tool for data assimilation into an almost steady model state. J. Phys. Oceanogr., *23,* 679–688.

Large, W. G., J. C. McWilliams and P. P. Niiler. 1986. Upper ocean thermal response to strong autumnal forcing of the northeast Pacific. J. Phys. Oceanogr., *16,* 1524–1550.

LeBrasseur, R. J. and O. D. Kennedy. 1972. Microzooplankton in coastal and oceanic areas of the Pacific Subarctic water mass: a preliminary report, *in* Biological Oceanography of the Northern Pacific Ocean, A. Y. Takenouti, ed., Idemitsu Shoten, Tokyo, 355–365.

Marotzke, J. 1992. The role of integration time in determining a steady state through data assimilation. J. Phys. Oceanogr., *12,* 1556–1567.

McAllister, C. D. 1961. Zooplankton studies at Ocean Weather Station P in the northeast Pacific Ocean. J. Fish. Res. Bd. Can., *18,* 1–29.

—— 1969. Aspects of estimating zooplankton production from phytoplankton production. J. Fish Res. Bd. Can., *26,* 199–220.

Metropolis, N., A. W. Rosenbluth, M. N. Rosenbluth, A. H. Teller and E. Teller. 1953. Equation of state calculations by fast computing machines. J. Chem. Phys., *21,* 1087–1092.

Miller, C. B., B. W. Frost, H. P. Batchelder, M. J. Clemons and R. E. Conway. 1984. Life histories of large, grazing copepods in a subarctic ocean gyre: *Neocalanus plumchrus, Neocalanus cristatus,* and *Eucalanus bungii* in the Northeast Pacific. Prog. Oceanogr., *13,* 201–243.

Parslow, J. S. 1981. Phytoplankton-zooplankton interactions: data analysis and modelling (with particular reference to Ocean Station P [50N, 145W] and controlled ecosystem experiments), Ph.D. thesis, University of British Columbia, 400 pp.

Parson, T. R. and C. M. Lalli. 1988. Comparative oceanic ecology of the plankton communities of the subarctic Atlantic and Pacific oceans. Oceanogr. Mar. Biol. Annu. Rev., *26,* 317–359.

Peng, T.-H. and W. Broecker. 1991. Dynamical limitations on the Antarctic iron fertilization strategy. Nature, *349,* 227–229.

Platt, T., K. H. Mann and R. E. Ulanowicz. 1981. Mathematical models in biological oceanography, UNESCO Monogr. Oceanogr. Methodol. 7.

Radach, G. and A. Moll. 1993. Estimation of the variability of production by simulating annual cycles of phytoplankton in the central North Sea. Prog. Oceanogr., *31,* 339–419.

Sarmiento, J. L., M. J. Fasham, R. Slater, J. R. Toggweiler and H. Ducklow. 1989. The role of biology in the chemistry of CO_2 in the ocean, *in* Chemistry of the Greenhouse Effect, M. Farrell, ed., Lewis Pub., New York.

Simon, M., N. A. Welschmeyer and D. L. Kirchman. 1992. Bacterial production and the sinking flux of particulate organic matter in the subarctic Pacific. Deep-Sea Res., *39,* 1997–2008.

Smith, S. E. 1936. Environmental control of photosynthesis in the sea. Proc. Natl. Acad. Sci. U.S.A, *22,* 504–511.

Steele, J. H. 1974. The Structure of Marine Ecosystem, Harvard Univ. Press, Cambridge.

Stephens, K. 1964. Productivity measurements in the northeast Pacific with associated chemical and physical data, 1958–1964, No. Fish. Res. Bd. Can., Oceanogr. Limnol. Manus. Rep., *179.*

—— 1966. Primary production data from the northeast Pacific Ocean, January 1964 to December 1965. No. Fish. Res. Bd. Can., Oceanogr. Limnol. Manus. Rep., *209.*

—— 1968. Primary production data from the northeast Pacific Ocean, January 1966 to December 1967. No. Fish. Res. Bd. Can. Oceanogr. Limnol. Manus. Rep., *957.*

—— 1970. Primary production data from the northeast Pacific Ocean, January 1967 to December 1969. No. Fish. Res. Bd. Can., Oceanogr. Limnol. Manus. Rep., *1123.*

Tarantola, A. 1987. Inverse Problem Theory. Elsevier Science, New York, NY, 613 pp.

Thacker, W. C. 1987. Three lectures on fitting numerical models to observations, No. External report GKSS 87/E/65, GKSS-Forschungszentrum Geesthacht, GmbHGeesthacht, Federal Republic of Germany.

Tziperman, E. and W. C. Thacker. 1989. An optimal-control/adjoint-equations approach to studying the oceanic general circulation. J. Phys. Oceanogr., *19,* 1471–1485.

Vézina, A. F. 1989. Construction of flow networks using inverse methods, *in* Network Analysis in Marine Ecology, F. Sulff *et al.,* eds., Springer-Verlag, 62–81.

Vézina, A. F. and T. Platt. 1988. Food web dynamics in the ocean. I. Best-estimates of flow networks using inverse methods. Mar. Ecol. Prog. Ser., *42,* 269–287.

Wheeler, P. A. and S. A. Kokkinakis. 1990. Ammonium recycling limits nitrate use in the oceanic subartic Pacific. Limnol. Oceanogr., *35,* 1267–1278.

Received: *29 August, 1994;* revised: *1 March, 1995.*